Diagnosis of Array Antennas Using Eigenmode Currents and Near-Field Data

Keisuke Konno, *Member, IEEE*, Shohei Asano, Tetsuya Umenai, and Qiang Chen, *Senior Member, IEEE*

***Abstract*— A novel method for the diagnosis of array antennas is proposed in this paper. The current distribution of the array antennas is reconstructed by the proposed method, which is based on the eigenmode currents over the entire array antennas and its near-field data. The eigenmode currents over the entire array antennas are numerically obtained via the method of moments. Only the dominant eigenmode currents are used for the reconstruction of the current distribution of the array antennas to alleviate the ill-posed nature of an inverse problem. The current distribution of the array antennas is reconstructed using the proposed method, and the optimum parameters for the proposed method, i.e., the number of dominant eigenmode currents and the length of a cylindrical scanning surface, are clarified. Finally, the proposed method is applied to the diagnosis of array antennas with abnormal excitations.**

***Index Terms*— Antenna diagnosis, eigenmode currents, inverse problem, method of moments (MoM), source reconstruction.**

I. Introduction

ACCORDING to recent advances in modern high-speed wireless communication systems, antenna technologies in the systems have been very complicated. For example, multiple antenna elements and beamforming technologies are indispensable for the next-generation wireless communication systems [1], [2]. The high-speed wireless communication systems are available based on such antenna technologies only when both of the antenna elements and their feed network operate as expected. On the other hand, the antenna elements or their feeds can be broken during operation, and maintenance is expected to be performed immediately. However, the maintenance of antenna elements or their feeds is costly, and services are stopped during maintenance. Therefore, it should be clarified whether or not antenna elements and their feeds work well in advance of their maintenance.

The diagnosis of array antennas using their near-field (NF) distribution is one of the promising approaches for finding problems on the array antennas. In general, the diagnosis of the array antennas can be performed via the reconstruction of equivalent sources or the current distribution of the array antennas themselves.

Manuscript received May 11, 2018; revised July 26, 2018; accepted August 2, 2018. Date of publication August 22, 2018; date of current version October 29, 2018. This work was supported by JSPS KAKENHI under Grant 18K13736. *(Corresponding author: Keisuke Konno.)*

K. Konno, T. Umenai, and Q. Chen are with the Department of Communications Engineering, Tohoku University, Sendai 980-8579, Japan (e-mail: konno@ecei.tohoku.ac.jp).

S. Asano is with Japan Post Corporation, Tokyo, Japan.

Color versions of one or more of the figures in this paper are available online at http://ieeexplore.ieee.org.

Digital Object Identifier 10.1109/TAP.2018.2866544

An NF to far-field transformation technique, which is based on reconstructed equivalent magnetic currents on a specific surface, has been proposed [3]. The technique uses an integral equation approach to reconstruct equivalent magnetic currents using complex electric fields measured over a rectangular surface. A reconstruction of equivalent electric/magnetic currents over more complicated surfaces has also been performed for practical antennas [4]. Alternatively, an optimization approach based on a conjugate gradient method has been proposed [5]. This approach reconstructs equivalent magnetic currents from phaseless electric fields and uses an iterative approach using a fast Fourier transform. The approach has been extended to applications regarding the reconstruction of equivalent magnetic currents over an arbitrary plane [6]. The current distribution of low directivity antennas has been reconstructed to obtain their far-field patterns [7]. These approaches have mainly been focused on the far-field pattern from reconstructed sources and not focused on the reconstruction of the current distribution of the array antennas themselves.

A novel backward transformation technique has been proposed, and an NF-to-NF transformation has been performed to detect a defective element in array antennas [8]. The backward transformation technique excludes evanescent wave components from the measured NF, because the components degrade the reconstructed aperture field. As a result, it has been shown that the defective element in the array antennas can be detected via the reconstructed aperture field. The NF distribution inside a scanning surface has been successfully obtained via an NF-to-NF transformation technique, and the so-called safety perimeter of the base station terminal antennas has been predicted [9]. The current distribution of a microstrip line on a multilayer printed circuit board has been reconstructed using a finite-difference time-domain method and an integral equation approach [10], [11]. In these studies, the measurement parameters were optimized and the current distribution of the microstrip line with lumped elements was successfully reconstructed. In recent years, a so-called compressive sensing (CS) approach has been introduced for the diagnosis of array antennas [12], [13]. For most of the practical array antennas, it can be assumed that the number of defective elements is much fewer than the total number of elements. The CS approach takes advantage of the sparsity of the defective elements in array antennas and enables the efficient performance diagnosis of array antennas.

One of the major problems regarding the diagnosis of array antennas is its ill-posed nature. To alleviate its ill-posed nature, the so-called regularization techniques have been proposed.

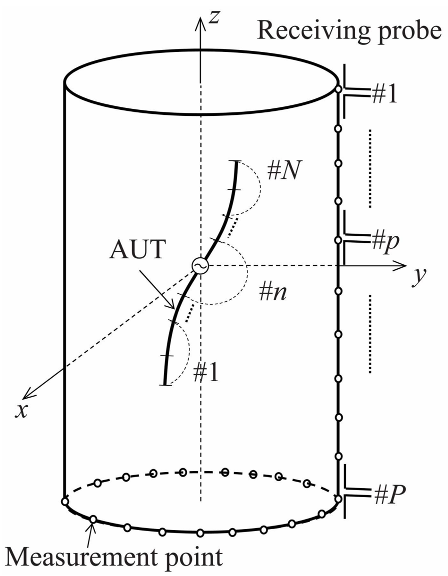

Fig. 1. AUT.

The Tikhonov regularization technique has been applied, and the equivalent magnetic currents of a patch antenna were successfully reconstructed in the presence of noise and measurement errors [14]. The effect of a penalty term on a regularization has been demonstrated via the source reconstruction of a digital printed circuit board [15]. A multiplicatively regularized source reconstruction method has been proposed and applied to the diagnosis of array antennas with deactivated elements [16]. These regularization techniques are based on purely mathematical techniques and alleviate the ill-posed nature of the problem. To the best of our knowledge, an approach using the eigenmode current of array antennas has not been applied to alleviate the ill-posed nature of the problem.

In this paper, a source reconstruction technique using the eigenmode currents of array antennas is proposed. The eigenmode currents of the array antennas are obtained from an impedance matrix calculated using the method of moments (MoM). Only dominant eigenmode currents are left and the remaining eigenmode currents, whose contributions to the current distribution are relatively small, are discarded. The unknown coefficients of the eigenmode currents are obtained using an integral equation approach and the measured NF distribution on a cylindrical scanning surface. The ill-posed nature of the matrix equation to be solved is alleviated, because the number of eigenmode currents used for the source reconstruction is reduced. The proposed method is applied to the source reconstruction of the array antennas, and optimum parameters for the proposed method are clarified. The results of numerical simulations and measurements demonstrate the performance of the proposed method for the diagnosis of array antennas with abnormal excitation.

II. Proposed Method

Fig. 1 shows an antenna under test (AUT) and a receiving probe. The receiving probe scans the cylindrical surface enclosing the AUT and measures the complex electric fields at specific points. Notably, the scanning surface can be any closed surface.

A. Eigenmode Currents

In advance of the source reconstruction, the eigenmode currents of the AUT should be obtained numerically. Here, the eigenmode currents of the AUT are obtained in the same manner as shown in [17]–[20]. According to the MoM, an $N \times N$ matrix equation is obtained [21], [22]

$$\mathbf{ZI} = \mathbf{V} \tag{1}$$

where $\mathbf{Z}$ is the $N \times N$ known impedance matrix of the AUT, $\mathbf{I}$ is an unknown N-dimensional current vector of the AUT to be reconstructed, $\mathbf{V}$ is the known N-dimensional voltage vector, and N is the total number of unknowns of the AUT. Notably, (1) only includes the AUT but not the receiving probe. Once the conjugate transpose of $\mathbf{Z}$ is multiplied by both sides of (1) from the left, the following matrix equation is available:

$$\mathbf{Z}^\dagger\mathbf{ZI} = \mathbf{Z}^\dagger\mathbf{V} \tag{2}$$

where $\dagger$ indicates the conjugate transpose. $\mathbf{Z}^\dagger\mathbf{Z}$ is a so-called Hermitian matrix, and its eigenvectors are orthogonal to each other. Therefore, the eigenvectors of $\mathbf{Z}^\dagger\mathbf{Z}$ are used as the eigenmode currents of the AUT.

B. Source Reconstruction

According to the orthogonality of the eigenmode currents, the unknown currents of the AUT can be expressed using the eigenmode currents as follows:

$$\mathbf{I}_N \approx \sum_{l=1}^{L} a_l \mathbf{e}_l \tag{3}$$

where $\mathbf{e}_l$ is an N-dimensional lth eigenmode current of the AUT, a_l is its unknown coefficient to be obtained, and $L(\leq N)$ is the total number of eigenmode currents used as basis functions. A specific L should be given in advance of the source reconstruction. One simple approach is to only keep L eigenmode currents whose eigenvalues are relatively small, because the contribution of an eigenmode current to the current is inversely proportional to its eigenvalue [17].

To obtain the unknown coefficients a_l $(l = 1, 2, \ldots, L)$, a matrix equation is formulated. As shown in Fig. 1, a receiving probe scans a cylindrical surface enclosing the AUT and measures the complex electric fields at P sampling points. The resultant receiving voltages are stored in a P-dimensional voltage vector $\mathbf{V}_P$. Afterward, a $P \times N$ mutual impedance matrix between the AUT and the receiving probe is obtained using the MoM as follows:

$$\mathbf{Z}_{P\times N} = \begin{bmatrix} Z_{11} & & \cdots & & Z_{1N} \\ & \ddots & & & \\ \vdots & & Z_{pn} & & \vdots \\ & & & \ddots & \\ Z_{P1} & & \cdots & & Z_{PN} \end{bmatrix} \tag{4}$$

where Z_{pn} is a mutual impedance between the receiving probe at the pth sampling point and the nth segment on the AUT. As a result, the following matrix equation is obtained:

$$\mathbf{Z}_{P\times N}\mathbf{I}_N = \mathbf{V}_P. \tag{5}$$

Equation (3) is substituted into (5), and the following matrix equations are obtained:

$$\begin{aligned}\mathbf{Z}_{P\times N}\sum_{l=1}^{L} a_l\mathbf{e}_l &= \mathbf{V}_P\\ \sum_{l=1}^{L} a_l\ (\mathbf{Z}_{P\times N}\mathbf{e}_l) &= \mathbf{V}_P\\ \mathbf{Z}'_{P\times L}\mathbf{a}_L &= \mathbf{V}_P\end{aligned} \tag{6}$$

where

$$\mathbf{Z}'_{P\times L} = \begin{bmatrix} \sum_{n=1}^{N} Z_{1n}e_{1n} & \sum_{n=1}^{N} Z_{1n}e_{2n} & \cdots & \sum_{n=1}^{N} Z_{1n}e_{Ln} \\ \vdots & \vdots & \ddots & \vdots \\ \sum_{n=1}^{N} Z_{Pn}e_{1n} & \sum_{n=1}^{N} Z_{Pn}e_{2n} & \cdots & \sum_{n=1}^{N} Z_{Pn}e_{Ln} \end{bmatrix} \tag{7}$$

$$\mathbf{a}_L = \begin{bmatrix} a_1 \\ \vdots \\ a_L \end{bmatrix}. \tag{8}$$

$\mathbf{Z}'_{P\times L}$ is a $P \times L$ matrix, Z_{pn} is a matrix element in the pth row and the nth column of $\mathbf{Z}_{P\times N}$, and e_{ln} is the nth component of the lth eigenmode current. Equation (6) can be solved using the singular value decomposition (SVD) or the pseudoinverse matrix, since $\mathbf{Z}'_{P\times L}$ is a rectangular matrix. The current distribution of the AUT is reconstructed from (3) and diagnosis of the AUT is performed.

In general, the condition number of a matrix becomes large as the size of the matrix increases, and the matrix with a large condition number suffers from numerical instability or poor accuracy. Therefore, the stability of the proposed method is expected to be improved when the number of eigenmode currents used for source reconstruction is reduced. The resultant current distribution of the AUT is expected to be reconstructed accurately, because practical antennas are usually designed to be excited by a single-mode current or the superposition of a couple of mode currents.

A conventional source reconstruction method using the MoM directly solves (5) using the SVD and its computational cost is $O(\min\{PN^2, P^2\ N\})$. On the other hand, the proposed method solves (6), which is available in advance of the source reconstruction when the number of dominant eigenmode currents L is known. The computational cost for solving (6) using the SVD is $O(\min\{PL^2, P^2\ L\})$. The ratio of the computational cost of the proposed method to that of the conventional method is tabulated in Table I. According to Table I, the ratio ranges from (L^2/N^2) to (L/N). Therefore, the computational cost of the proposed method decreases as the square of (L/N) for the best case, while the cost decreases in proportion to (L/N) for the worst case.

TABLE I

COMPUTATIONAL COST OF THE PROPOSED AND THE CONVENTIONAL METHOD

	$P \geq N(\geq L)$	$L \leq P < N$	$P < L < N$
Conventional	PN^2	P^2N	P^2N
Proposed	PL^2	PL^2	P^2L
Ratio	$\frac{L^2}{N^2}$	$\frac{L^2}{PN}$	$\frac{L}{N}$

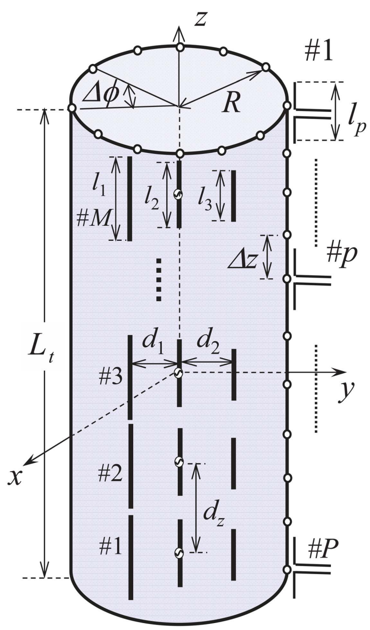

Fig. 2. Yagi–Uda array antennas.

Finally, a flowchart of the proposed method is summarized as follows.

1) The eigenmode currents of the AUT are obtained numerically via the MoM.
2) The receiving probe measures the complex electric fields on the cylindrical scanning surface and its receiving voltages are stored to $\mathbf{V}_P$.
3) A $P \times N$ mutual impedance matrix $\mathbf{Z}_{P\times N}$ between the AUT and the receiving probe is obtained numerically via the MoM.
4) The unknown coefficients of the eigenmode currents are obtained via the SVD.
5) According to (3), the current distribution of the AUT is reconstructed.
6) From the reconstructed current distribution, a diagnosis of the AUT is performed.

Notably, the proposed method is applicable to the source reconstruction of the AUT with a nonuniform excitation, because no assumption is made for the excitation of the AUT during its formulation.

III. NUMERICAL SIMULATION

The performance of the proposed method is demonstrated by numerical simulation. Two numerical examples are shown in Figs. 2 and 3. Parameters for the source reconstruction of them are shown in Tables II and III. The first example

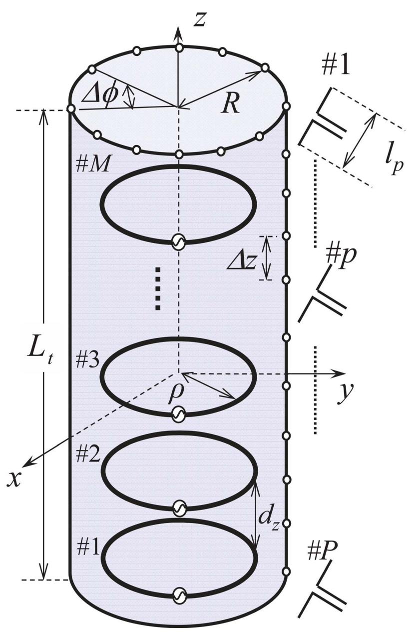

Fig. 3. Loop array antennas.

TABLE II

PARAMETERS FOR THE SOURCE RECONSTRUCTION OF YAGI–UDA ARRAY ANTENNAS

Frequency	$f = 1$ GHz
Length of reflector	$l_1 = 0.6\lambda$
Length of radiator	$l_2 = 0.5\lambda$
Length of director	$l_3 = 0.4\lambda$
Radius of elements	$a = 0.0033\lambda$
Spacing between reflector and radiator	$d_1 = 0.25\lambda$
Spacing between radiator and director	$d_2 = 0.25\lambda$
Array spacing	$d_z = 0.65\lambda$
Number of antenna elements	$M = 10$
Number of segments in single element	$K = 15$
Total number of segments	$N = MK = 150$
Length of receiving probe	$l_p = 0.1\lambda$

TABLE III

PARAMETERS FOR THE SOURCE RECONSTRUCTION OF LOOP ARRAY ANTENNAS

Frequency	$f = 1$ GHz
Radius of loop element	$\rho = \frac{\lambda}{2\pi}$
Radius of elements	$a = 0.0033\lambda$
Array spacing	$d_z = 0.65\lambda$
Number of antenna elements	$M = 5$
Number of segments in single element	$K = 11$
Total number of segments	$N = MK = 55$
Length of receiving probe	$l_p = 0.1\lambda$

uses Yagi–Uda array antennas, and the second one employs loop array antennas. Both of the array antennas have uniform amplitudes and in-phase excitations. A receiving probe scans the cylindrical surface enclosing the AUT, the length of the scanning cylinder is L_t [λ], and the radius of the scanning cylinder is R [λ]. The measurement interval of the receiving probe is Δz [λ] for the z direction and $\Delta\phi$ [deg.] for the ϕ direction. The resulting number of total measurement points is P. The polarization of the receiving probe corresponds to that of the AUT, namely, E_z for the Yagi–Uda array antennas and E_ϕ for the loop array antennas. All numerical simulations in this paper are performed using Richmond's MoM [21], [22]. White noise is added to the measured voltage so that the dynamic range of the measurement system is maintained.

A correlation function is introduced to evaluate the performance of the proposed method

$$\gamma = \frac{\left|\sum_{n=1}^{N}(|I_n| - \overline{|I|})(|I'_n| - \overline{|I'|})\right|}{\sqrt{\sum_{n=1}^{N}(|I_n| - \overline{|I|})^2}\sqrt{\sum_{n=1}^{N}(|I'_n| - \overline{|I'|})^2}} \tag{9}$$

where I_n and I'_n are the reconstructed and calculated current of the nth segment, respectively, and $\overline{|I_n|}$ and $\overline{|I'_n|}$ indicate the average of their amplitudes.

A condition number is also introduced to evaluate the stability of the proposed method

$$\kappa = \frac{\sigma_{\max}}{\sigma_{\min}} \tag{10}$$

where $\sigma_{\min}$ and $\sigma_{\max}$ are the minimum and the maximum singular values of $\mathbf{Z}'_{P\times L}$, respectively.

A. Parameter Study

Fig. 4 shows the effect of the number of eigenmode currents on the correlation function and the condition number. As expected in Section II-B, the condition number decreases as the number of eigenmode currents used for source reconstruction decreases. In contrast, the correlation function gradually approaches unity as the number of eigenmode currents decreases to a moderate value. The proposed method reconstructs the current of the AUT using eigenmode currents and receiving voltages, which are a sum of the voltages produced by each eigenmode current. As previously mentioned, the eigenmode currents that correspond to relatively large eigenvalues exhibit a small contribution to the current of the AUT. Therefore, it is difficult to accurately reconstruct coefficients of such eigenmode currents, because their contribution to receiving voltages is too small and sometimes not available. Although the number of eigenmode currents should be reduced in advance of the source reconstruction, the dominant eigenmode currents should be kept. According to Fig. 4, the number of eigenmode currents can be reduced from N to the number of isolated elements without degrading the accuracy. For example, $L = 30(=3M)$ and $L = 5(=M)$ are the optimized values for the Yagi–Uda array antennas and the loop array antennas, respectively.

Fig. 5 shows the effect of the length of the scanning cylinder L_t on the correlation function and condition number. It is found that the condition number converges to the minimum when the scanning cylinder completely encloses the AUT, namely, $L_t > 6.45\lambda$ for the Yagi–Uda array antennas and $L_t > 2.7\lambda$ for the loop array antennas. In addition, the condition number of $\mathbf{Z}'_{P\times L}$ obtained for the same L_t becomes quite small by one or two orders of magnitude when the number of eigenmode currents is reduced from the total number of unknowns N to the total number of isolated elements. Moreover, the correlation function quickly converges to unity as the length of scanning cylinder L_t increases when the number of

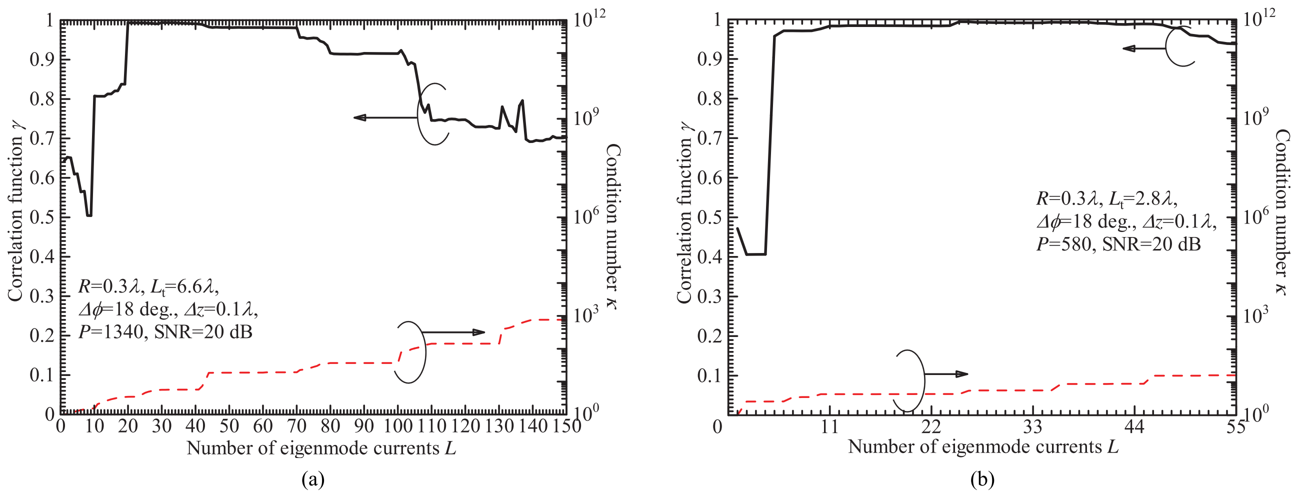

Fig. 4. Effect of the number of the eigenmode currents on the correlation function and condition number. (a) Yagi–Uda array antennas. (b) Loop array antennas.

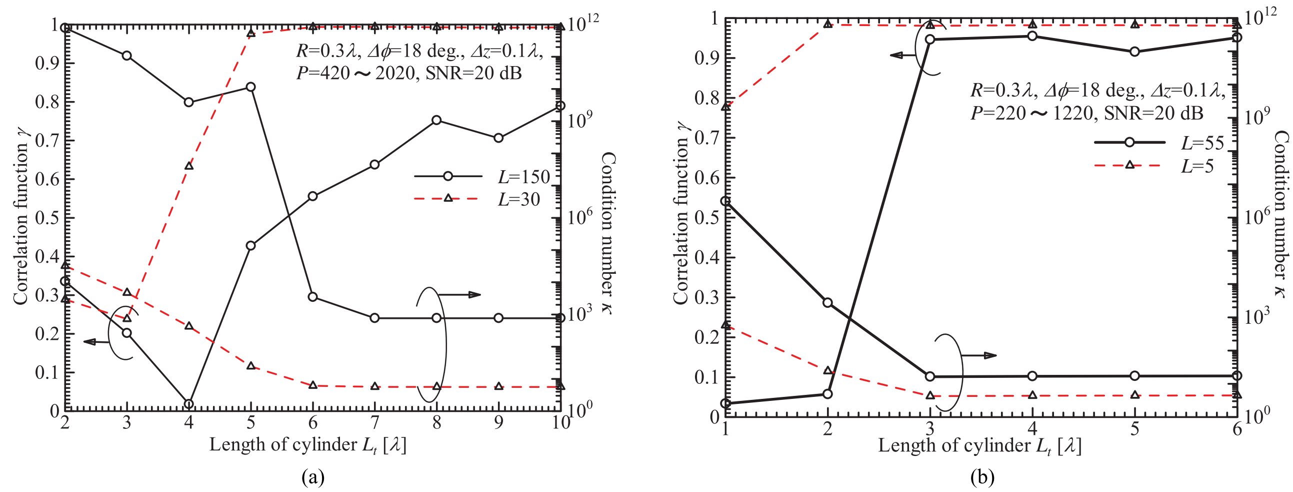

Fig. 5. Effect of the length of the scanning cylinder on the correlation function and condition number. (a) Yagi–Uda array antennas. (b) Loop array antennas.

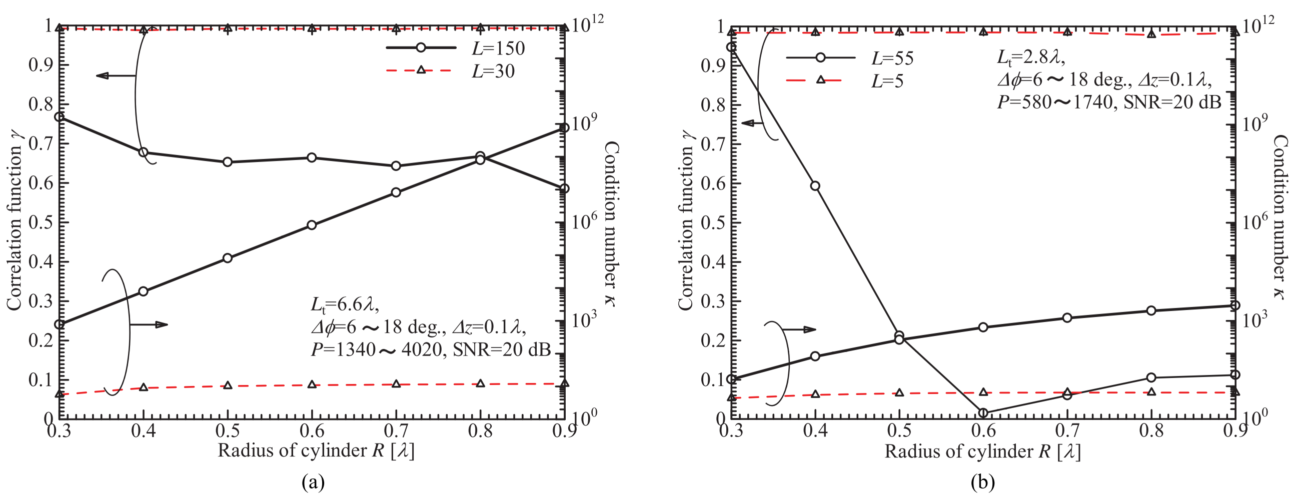

Fig. 6. Effect of the radius of the scanning cylinder on the correlation function and condition number. (a) Yagi–Uda array antennas. (b) Loop array antennas.

eigenmode currents is reduced. Therefore, it can be concluded that a reduction in the number of eigenmode currents can quite effectively enhance the stability and accuracy of the proposed method.

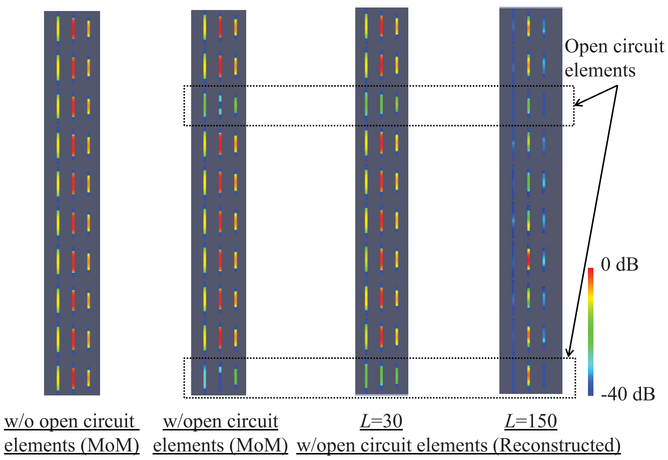

Fig. 7. Current distribution of the Yagi–Uda array antennas with two open-circuit elements ($L_t = 6.6\lambda$, $R = 0.3\lambda$, $\Delta z = 0.1\lambda$, $\Delta\phi = 18$ deg., $P = 1340$, and SNR $= 20$ dB).

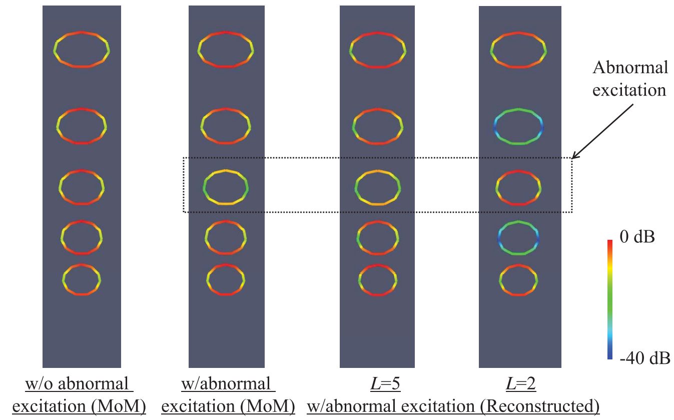

Fig. 8. Current distribution of the loop array antennas with abnormal excitation ($L_t = 2.8\lambda$, $R = 0.3\lambda$, $\Delta z = 0.1\lambda$, $\Delta\phi = 18$ deg., $P = 580$, and SNR $= 20$ dB).

Fig. 6 describes the effect of the radius of the scanning cylinder on the correlation function and condition number. As clearly demonstrated, the condition number increases as the radius of the scanning cylinder increases, especially when all the eigenmode currents are used. The proposed method is categorized as the so-called NF-to-NF transformation technique, and the NF measured on the cylindrical scanning surface includes an evanescent wave, which is exponentially attenuated. It is difficult to measure such an evanescent wave because of its small amplitude and measurement error. In particular, the evanescent wave produced by the eigenmode currents that correspond to relatively large eigenvalues is difficult to measure, because its contribution to the AUT currents, which is the source of the evanescent wave, is so small. As a result, the source reconstruction via the proposed method becomes an ill-posed problem as the radius of the scanning cylinder increases when the all the eigenmode currents are used. Alternatively, as shown in Fig. 6, both the condition number and correlation function are almost independent of the radius of the scanning cylinder when the number of eigenmode currents is reduced. It can be said that the ill-posed nature of the source reconstruction is alleviated due to a reduction in the number of eigenmode currents even when the radius of the scanning cylinder increases.

B. Diagnosis of Array Antennas

The diagnosis of array antennas is performed using the proposed method. The first example employs the Yagi–Uda array antennas that include two open-circuit elements. Fig. 7 shows the reconstructed current of the Yagi–Uda array antennas. It is found that two open-circuit elements are clearly visible when $L = 30$, while they are not when $L = 150$. Owing to the reduction in the number of eigenmode currents, the condition number of the problem decreases, and the current distribution of the Yagi–Uda array antennas is successfully reconstructed when $L = 30$. On the other hand, the current distribution of the Yagi–Uda array antennas is erroneous when $L = 150$ because of the high condition number. The second example uses the loop array antennas, including one abnormally excited

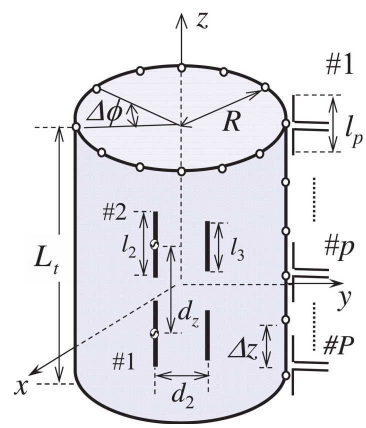

Fig. 9. Two element Yagi–Uda array antenna.

element. It is assumed that all array elements are uniformly excited by a voltage source of 1 V, except for the central one. The central element is excited by the voltage source of 0.1 V. Fig. 8 shows the reconstructed current of the loop array antennas. It is found that one abnormally excited element is clearly seen when $L = 5$, while it is not when $L = 2$. According to these numerical results, it can be concluded that a moderate number of eigenmode currents, i.e., the number of isolated elements, should be used for the successful source reconstruction of array antennas.

IV. Measurement Results

Finally, the NF of a two-element Yagi–Uda array antenna shown in Fig. 9 is measured, and its current distribution is reconstructed. The measurement system is shown in Fig. 10, while the fabricated AUT and a probe are shown in Fig. 11. The AUT is on a turntable, and the probe is mounted on a positioner. The probe is a small dipole antenna with a balun, and its length is 0.1λ at 2 GHz. The complex NF of the AUT was measured on a cylindrical scanning surface using a network analyzer. To perform diagnosis of the AUT, element #1 is excited, but element #2 is only terminated with a 50-Ω load. Parameters for the source reconstruction of the AUT are tabulated in Table IV. As shown in Fig. 9, the balun and coaxial cables are neglected during the source reconstruction. Due to the limitation of our measurement

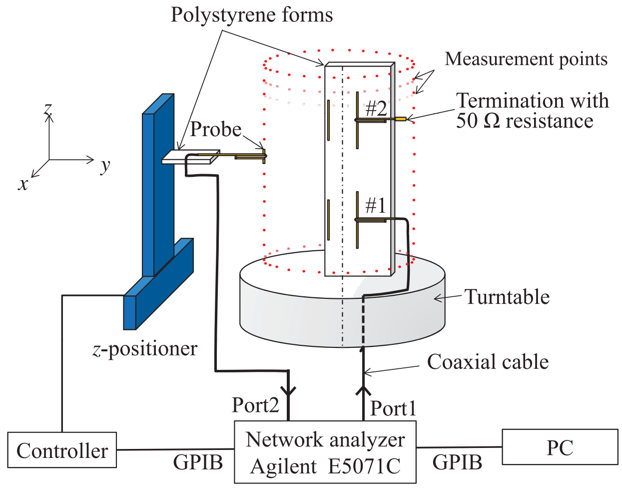

Fig. 10. Measurement system.

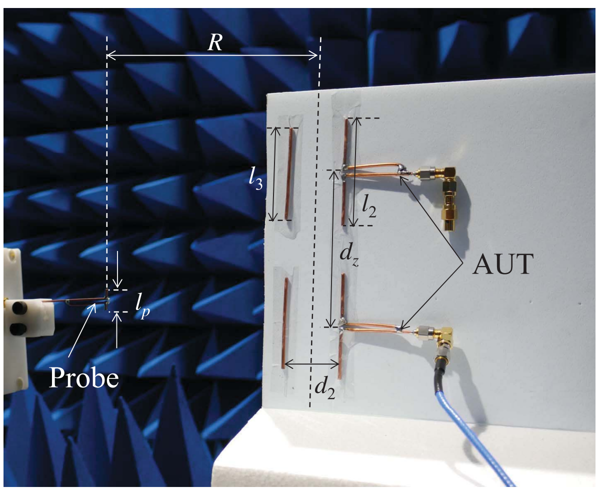

Fig. 11. Picture of AUT and probe.

TABLE IV

Parameters for the Source Reconstruction of Two Element Yagi–Uda Array Antenna

Frequency	$f = 2$ GHz
Length of radiator	$l_2 = 0.44\lambda$
Length of director	$l_3 = 0.39\lambda$
Radius of elements	$a = 0.0033\lambda$
Spacing between radiator and director	$d_2 = 0.23\lambda$
Array spacing	$d_z = 0.65\lambda$
Number of antenna elements	$M = 2$
Number of segments in single element	$K = 10$
Total number of segments	$N = MK = 20$
Length of receiving probe	$l_p = 0.1\lambda$
Length of scanning cylinder	$L_t = 1.3\lambda$
Radius of scanning cylinder	$R = \lambda$
Measurement interval in z-direction	$\Delta z = 0.1\lambda$
Measurement interval in ϕ-direction	$\Delta\phi = 12$ deg.
Number of measurement points	$P = 420$

system, the radius of the scanning cylinder was 150 mm (1λ at 2 GHz).

The current distribution of the AUT obtained using the MoM and the reconstructed using the proposed method is shown in Fig. 12. The complex NF measured on the cylindrical scanning surface was used for the reconstruction of the current distribution. It is found that an element with abnormal excitation is clearly visible from the reconstructed current when

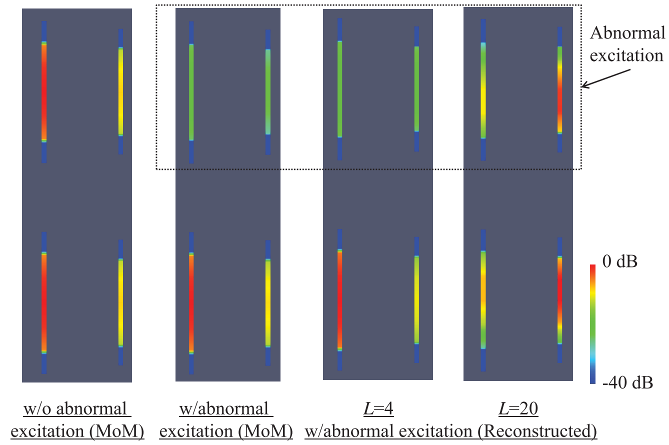

Fig. 12. Current distribution of the two-element Yagi–Uda array antenna with abnormal excitation.

$L = 4$, while they are not when $L = 20$. As previously discussed, the condition number of the problem decreases when the number of eigenmode currents is reduced to a moderate value. As a result, the current distribution of the AUT is successfully reconstructed using the proposed method, and the diagnosis of the AUT works well. In contrast, the current distribution of the AUT is erroneous when $L = 20$ because of the high condition number. It can be concluded that the proposed method is an effective technique for the diagnosis of the AUT.

V. Conclusion

In this paper, a novel source reconstruction technique has been proposed. The proposed method reconstructs the current distribution of an AUT using its eigenmode currents and complex NF measured on a cylindrical scanning surface. Numerical simulations clarify that the number of eigenmode currents should be reduced to a moderate value for the successful source reconstruction. The effect of the length and radius of the cylindrical scanning surface on the accuracy of the proposed method has been clarified. The proposed method has been applied to the diagnosis of array antennas. Owing to the proposed method with a moderate number of eigenmode currents, a defective element, such as an open-circuit element or an element with abnormal excitation, is found. Finally, the proposed method has been applied to the diagnosis of fabricated array antennas. The source reconstruction was performed using the measured complex NF around the fabricated array antennas, and an element with an abnormal excitation has been found successfully.

It should be indicated that one of the main focuses of this paper is to clearly demonstrate a methodology of the proposed method. Therefore, in this paper, source reconstruction has been performed for simplified free-standing array antennas although the proposed method is applicable to the source reconstruction of more complicated structures. The optimum parameters of the proposed method for source reconstruction of the AUT, including more complicated structures, are expected to be available in the same manner at the expense of computational cost.

Acknowledgment

The authors would like to thank the staff at the Cyberscience Center, Tohoku University, for their helpful advice.

References

[1] H. Papadopoulos, C. Wang, O. Burasalioglu, X. Hou, and Y. Kishiyama, "Massive MIMO technologies and challenges towards 5G," *IEICE Trans. Commun.*, vol. E99-B, no. 3, pp. 602–621, Mar. 2016.

[2] O. Jo, J.-J. Kim, J. Yoon, D. Choi, and W. Hong, "Exploitation of dual-polarization diversity for 5G millimeter-wave MIMO beamforming systems," *IEEE Trans. Antennas Propag.*, vol. 65, no. 12, pp. 6646–6655, Dec. 2017.

[3] P. Petre and T. K. Sarkar, "Planar near-field to far-field transformation using an equivalent magnetic current approach," *IEEE Trans. Antennas Propag.*, vol. 40, no. 11, pp. 1348–1356, Nov. 1992.

[4] L. J. Foged, L. Scialacqua, F. Saccardi, J. L. A. Quijano, G. Vecchi, and M. Sabbadini, "Practical application of the equivalent source method as an antenna diagnostics tool [AMTA Corner]," *IEEE Antennas Propag. Mag.*, vol. 54, no. 5, pp. 243–249, Oct. 2012.

[5] F. Las-Heras and T. K. Sarkar, "A direct optimization approach for source reconstruction and NF-FF transformation using amplitude-only data," *IEEE Trans. Antennas Propag.*, vol. 50, no. 4, pp. 500–510, Apr. 2002.

[6] Y. Alvarez, F. Las-Heras, and M. R. Pino, "The sources reconstruction method for amplitude-only field measurements," *IEEE Trans. Antennas Propag.*, vol. 58, no. 8, pp. 2776–2781, Aug. 2010.

[7] Z. Ouardirhi and J. J. Laurin, "Near-field characterization of low directivity wire antennas," in *Proc. URSI Int. Symp. Electromagn. Theory*, May 2001, pp. 229–231.

[8] J. J. Lee, E. M. Ferren, D. P. Woollen, and K. M. Lee, "Near-field probe used as a diagnostic tool to locate defective elements in an array antenna," *IEEE Trans. Antennas Propag.*, vol. AP-36, no. 6, pp. 884–889, Jun. 1988.

[9] A. Ziyyat, L. Casavola, D. Picard, and J. C. Bolomey, "Prediction of BTS antennas safety perimeter from NF to NF transformation: An experimental validation," in *Proc. AMTA*, Oct. 2001, pp. 22–26.

[10] Q. Chen, S. Kato, and K. Sawaya, "Estimation of current distribution on multilayer printed circuit board by near-field measurement," *IEEE Trans. Electromagn. Compat.*, vol. 50, no. 2, pp. 399–405, May 2008.

[11] S. Kato, Q. Chen, and K. Sawaya, "Current estimation on multi-layer printed circuit board with lumped circuits by near-field measurement," *IEICE Trans. Commun.*, vols. E91–B, no. 11, pp. 3788–3791, Nov. 2008.

[12] B. Fuchs, L. Le Coq, and M. D. Migliore, "Fast antenna array diagnosis from a small number of far-field measurements," *IEEE Trans. Antennas Propag.*, vol. 64, no. 6, pp. 2227–2235, Jun. 2016.

[13] A. F. Morabito, R. Palmeri, and T. Isernia, "A compressive-sensing-inspired procedure for array antenna diagnostics by a small number of phaseless measurements," *IEEE Trans. Antennas Propag.*, vol. 64, no. 7, pp. 3260–3265, Jul. 2016.

[14] J. Colinas, Y. Goussard, and J. J. Laurin, "Application of the Tikhonov regularization technique to the equivalent magnetic currents near-field technique," *IEEE Trans. Antennas Propag.*, vol. 52, no. 11, pp. 3122–3132, Nov. 2004.

[15] P. A. Barrière, J.-J. Laurin, and Y. Goussard, "Mapping of equivalent currents on high-speed digital printed circuit boards based on near-field measurements," *IEEE Trans. Electromagn. Compat.*, vol. 51, no. 3, pp. 649–658, Aug. 2009.

[16] T. Brown, I. Jeffrey, and P. Mojabi, "Multiplicatively regularized source reconstruction method for phaseless planar near-field antenna measurements," *IEEE Trans. Antennas Propag.*, vol. 65, no. 4, pp. 2020–2031, Apr. 2017.

[17] D. J. Bekers, S. J. L. van Eijndhoven, A. A. F. van de Ven, P.-P. Borsboom, and A. G. Tijhuis, "Eigencurrent analysis of resonant behavior in finite antenna arrays," *IEEE Trans. Microw. Theory Techn.*, vol. 54, no. 6, pp. 2821–2829, Jun. 2006.

[18] D. J. Bekers, S. J. L. van Eijndhoven, and A. G. Tijhuis, "An eigencurrent approach for the analysis of finite antenna arrays," *IEEE Trans. Antennas Propag.*, vol. 57, no. 12, pp. 3772–3782, Dec. 2009.

[19] V. Lancellotti, B. P. de Hon, and A. G. Tijhuis, "An eigencurrent approach to the analysis of electrically large 3-D structures using linear embedding via Green's operators," *IEEE Trans. Antennas Propag.*, vol. 57, no. 11, pp. 3575–3585, Nov. 2009.

[20] V. Lancellotti, B. P. de Hon, and A. G. Tijhuis, "On the convergence of the eigencurrent expansion method applied to linear embedding via Green's operators (LEGO)," *IEEE Trans. Antennas Propag.*, vol. 58, no. 10, pp. 3231–3238, Oct. 2010.

[21] R. F. Harrington, *Field Computation by Moment Methods*. New York, NY, USA: Macmillan, 1968.

[22] J. H. Richmond and N. Geary, "Mutual impedance of nonplanar-skew sinusoidal dipoles," *IEEE Trans. Antennas Propag.*, vol. AP-23, no. 3, pp. 412–414, May 1975.

Keisuke Konno (M'12) received the B.E., M.E., and D.E. degrees from Tohoku University, Sendai, Japan, in 2007, 2009, and 2012, respectively.

Since 2012, he has been with the Department of Communications Engineering, Graduate School of Engineering, Tohoku University, where he is currently an Assistant Professor. Since 2015, he has been with the ElectroScience Laboratory, The Ohio State University, Columbus, OH, USA, as a Visiting Scholar. His current research interests include computational electromagnetics, array antennas, and reflectarrays.

Dr. Konno is a member of the Institute of Electronics, Information and Communication (IEICE). He received the JSPS Post-Doctoral Fellowships for Research Abroad, the Encouragement Award for Young Researcher and the Most Frequent Presentations Award from the Technical Committee on Antennas and Propagation of Japan, in 2010, the Young Researchers Award from the IEICE of Japan, in 2011, the IEEE EMC Society Sendai Chapter Student Brush-up Session & EMC Sendai Seminar Student Best Presentation Award in 2011, and the JSPS Washington Director Award in 2016.

Shohei Asano received the B.E. and M.E. degrees from Tohoku University, Sendai, Japan, in 2016 and 2018, respectively.

He has been with Japan Post Corporation, Tokyo, Japan. His current research interests include electromagnetic inverse problems.

Tetsuya Umenai received the B.E. degree from Akita Prefectural University, Yurihonjo, Japan, in 2017. He is currently pursuing the M.E. degree with Tohoku University, Sendai, Japan.

His current research interests include electromagnetic inverse problems.

Qiang Chen (M'94–SM'12) received the B.E. degree from Xidian University, Xi'an, China, in 1986, and the M.E. and D.E. degrees from Tohoku University, Sendai, Japan, in 1991 and 1994, respectively.

He is currently a Chair Professor with the Electromagnetic Engineering Laboratory, Department of Communications Engineering, Faculty of Engineering, Tohoku University. His current research interests include antennas, microwave and millimeter wave, electromagnetic measurement, and computational electromagnetics.

Dr. Chen is a member of the Institute of Electronics, Information and Communication Engineers (IEICE). He received the Young Scientists Award in 1993 and the Best Paper Award and the Zen-ichi Kiyasu Award from the IEICE in 2009. He served as the Chair for the IEICE Technical Committee on Photonics-Applied Electromagnetic Measurement from 2012 to 2014 and the Vice Chair of the IEEE Antennas and Propagation Society Japan Chapter from 2012 to 2013. He is currently the Chair of the IEICE Technical Committee on Wireless Power Transfer. He was the Secretary and the Treasurer of the IEEE Antennas and Propagation Society Tokyo Chapter in 1998, the Secretary of the Technical Committee on Electromagnetic Compatibility of the IEICE from 2004 to 2006, and the Secretary of the Technical Committee on Antennas and Propagation of the IEICE from 2008 to 2010. He was an Associate Editor of the *IEICE Transactions on Communications* from 2007 to 2012.